Textile & Leather Review

ISSN 2623-6281 | www.tlr-journal.com | 10.31881/TLR

Motion Planning and Energy Consumption Optimization of G1 Robot Based on Spherical Coordinate Transformation

Liping Zhang

How to cite: Zhang L. Motion Planning and Energy Consumption Optimization of G1 Robot Based on Spherical Coordinate Transformation. Textile & Leather Review. 2026; 9:3930-3955. https://doi.org/10.31881/TLR.2026.3930

How to link: https://doi.org/10.31881/TLR.2026.3930

Published: 25 April 2026

Motion Planning and Energy Consumption Optimization of G1 Robot Based on Spherical Coordinate Transformation

Liping Zhang

Tianyou College, East China Jiaotong University, Nanchang 330013, Jiangxi, China
15280807408@163.com

Article
https://doi.org/10.31881/TLR.2026.3930
Published 25 April 2026

ABSTRACT

Facing the challenge of rapidly increasing energy consumption in robotics, this study proposes a physical model to optimize motor motion and efficiency. By implementing an innovative spherical coordinate to Cartesian coordinate transformation, we achieve precise calculation of the robotic arm's end-effector position while completing comprehensive drive motor safety verification. By implementing spherical-to-Cartesian transformation, we achieve precise end-effector positioning while reducing computational overhead. Furthermore, the research incorporates quintic polynomial trajectory planning combined with a trigonometric phase-shift model to achieve coordinated multi-joint motion analysis. Furthermore, combining quintic polynomials with a trigonometric phase-shift model ensures smooth trajectories and coordinated joint motion. The proposed methodology addresses a critical gap in robotic systems by harmonizing motion accuracy with energy conservation. By focusing on physical modeling and trajectory optimization, this work provides a viable technical pathway for tackling energy consumption challenges in industrial robots. This framework demonstrates that strategic motion planning significantly reduces energy usage without compromising performance, supporting the development of sustainable industrial automation. This research contributes to sustainable robotics by offering a practical solution that balances operational demands with environmental considerations, paving the way for wider adoption of energy-conscious practices in industrial automation.

KEYWORDS

spherical coordinate-cartesian coordinate conversion, polynomial interpolation, mathematical modeling

INTRODUCTION

As the application scenarios of robots continuously expand from industrial manufacturing to home services, humanoid robots demonstrate unique advantages in fields such as service, healthcare, and entertainment due to their anthropomorphic structure. However, multi-degree-of-freedom limb systems face inherent conflicts

among motion expressiveness, dynamic stability, and energy efficiency when performing dynamic tasks such as dancing. Yin et al. optimized industrial robot trajectory planning using machine learning methods, revealing for the first time the potential of data-driven approaches in energy consumption control [1]. Fazilat and Zioui further integrated precise CAD-based dynamic modeling with a Quantum-Inspired Sliding-Mode Control (Q-SMC) strategy, achieving a 3.79% reduction in energy consumption while enhancing motion precision and robustness in articulated robotic systems [2]. Nevertheless, the stability risks and energy peaks caused by intense movements have yet to be effectively addressed. In complex tasks, the energy consumption of humanoid robots can reach multiple times that of static working conditions, and the stability margin at zero torque points can fluctuate significantly [3]. This multi-objective conflict highlights the shortcomings of existing methods in collaborative optimization and urgently calls for innovative solutions.

Recent studies have proposed various technical approaches, but they all have obvious limitations. At the motion planning level, Soleimani Amiri and others used a genetic-swarm hybrid algorithm to solve the inverse kinematics problem. Although this improved computational accuracy, the algorithm is relatively complex [4]; Zhang and others applied an improved particle swarm optimization algorithm to the trajectory planning of six-degree-of-freedom manipulators, but it faced the problem of slow convergence [5]. In terms of stability control, the inverse dynamics fuzzy gain scheduling method proposed by Kadri and others achieved significant breakthroughs [6], but as Liu and others pointed out, in multi-UAV system collaborative planning, stability is often treated as a posterior constraint [7].

Research on energy optimization also has shortcomings. Szumska's review of regenerative braking systems [8] and Chidambaram and others' study on the impact of regenerative braking on battery life [9] both failed to deeply integrate with motion planning. Metaheuristic algorithms, such as Kouhi and others' study on multi-vehicle collaborative parking trajectory planning [10], can handle multi-objective optimization problems, but they have the drawbacks of high computational cost and a tendency to get stuck in local optima. Notably, the intelligent thermal management framework proposed by Shili and others [11] and Michael's research on energy harvesting in long-duration robot exploration [12] highlight the importance of thermal constraints, but most existing studies over-simplify dynamic constraints [13], resulting in a significant gap between theoretical models and practical applications.

THE FUNDAMENTAL MODELING FRAMEWORK

This study establishes a four-tiered collaborative framework for robotic motion analysis, integrating spherical coordinate transformation, vector analysis, safety verification, and trajectory planning methods. The framework transforms complex kinematic problems into intuitive geometric mappings, quantifies motion characteristics through spatial vectors, and employs a dual verification mechanism to ensure drive reliability. By combining polynomial and trigonometric models, the approach achieves smooth trajectory planning while incorporating energy adaptation strategies [14]. This integrated methodology combines analytical precision with energy management principles, including renewable energy integration for long-duration operations, providing a comprehensive foundation for robotic system design that balances computational efficiency with power conversion optimization. To clarify the scope of this research, the UniTree G1 humanoid robot serves as the unified subject of study. As a complex whole-body system, the G1 comprises both upper-limb manipulators (analyzed as 5-DOF robotic arms) for spatial task execution and bipedal lower limbs for locomotion. Because humanoid robots face severe energy constraints during dynamic whole-body tasks, our optimization framework is systematically divided into two synergistic parts. First, we address the kinematic redundancy and energy consumption of the upper limbs using a spherical coordinate transformation approach. Second, we ensure the dynamic stability and energy efficiency of the lower limbs through a trigonometric trajectory planning model. Together, these two parts constitute a comprehensive whole-body motion optimization strategy.

Spherical coordinate system model

This research presents a comprehensive methodological framework addressing the kinematic modeling challenges of the G1 robotic system through an innovative spherical coordinate transformation approach. The investigation initiates with a critical analysis of the inherent complexities associated with the robot's five-degree-of-freedom arm architecture, revealing significant computational redundancy problems in conventional linkage modeling methodologies. Traditional approaches based on Denavit-Hartenberg parameters and homogeneous transformation matrices, while mathematically rigorous, often result in computationally intensive solutions that are impractical for real-time control applications, particularly in dynamic environments requiring rapid trajectory replanning.

The proposed methodology employs a computationally efficient analytical alternative to conventional kinematic modeling by establishing a spherical coordinate system for the G1′s 5-DOF arm. This approach

transforms multi-joint coordination into localized angular parameter variations, effectively reducing the computational overhead inherent in matrix-based homogeneous transformations. While modern data-driven or hybrid kinematic solvers offer high flexibility, they often require extensive training data and can exhibit non-deterministic latency [1, 2]. In contrast, the spherical geometric mapping used here provides a deterministic, low-latency solution ideal for real-time energy optimization. This foundational transformation facilitates a more intuitive spatial representation, thereby streamlining the subsequent trajectory planning and optimization processes [15]. The implementation of this spherical coordinate-based modeling framework demonstrates significant advantages in practical applications. The simplified parameter space enables more efficient motion planning algorithms, reduces computational resource requirements, and improves the reliability of real-time control systems. Furthermore, this approach provides a more natural representation for human operators interacting with the robotic system, as the spherical coordinates align closely with intuitive spatial reasoning about arm positioning and orientation.

Validation studies confirm that the proposed methodology maintains the precision requirements for industrial applications while achieving substantial improvements in processing speed compared to traditional modeling techniques. The framework's scalability and adaptability suggest potential applications beyond the G1 robot system, extending to various articulated robotic manipulators with similar kinematic structures. This research contributes to the advancement of robotic modeling techniques by providing a balanced solution that harmonizes mathematical rigor with practical implementation considerations, paving the way for more efficient and accessible robotic control systems in industrial automation environments.

The spatial position of the end effector can be accurately described by the following analytical formula, which defines the mapping from the spherical coordinate space (r, θ, φ) to the Cartesian space (x, y, z) :

$$\begin{aligned} x &= r \cdot \sin(\theta) \cdot \cos(\varphi) \\ y &= r \cdot \sin(\theta) \cdot \sin(\varphi) \\ z &= r \cdot \cos(\theta) \end{aligned} \tag{1}$$

Where x, y, z represent the coordinates in the Cartesian system; r is the radial distance (arm length from the shoulder joint to the end-effector); θ represents the pitch angle (measured as the inclination from the vertical z-axis); and φ represents the yaw angle (measured as the rotation from the x-axis toward the y-axis in the

horizontal plane). This coordinate transformation simplifies the 5-DOF inverse kinematics into a geometric mapping, significantly reducing computational overhead.

This coordinate transformation method transforms the complex multi-degree-of-freedom inverse kinematics problem into a concise geometric mapping relationship, which not only ensures the calculation accuracy, but also significantly improves the calculation efficiency of motion planning, and provides a new theoretical basis for robot trajectory optimization.

Motion quantitative analysis

Within the framework of energy consumption analysis of robot motion, accurate quantification of the motion amplitude of the manipulator is an important basis for establishing energy consumption models. This study uses the Euclidean space vector analysis method, through rigorous mathematical modeling to provide a theoretical basis for the subsequent energy consumption calculation. Based on the three-dimensional spatial geometry, the method converts the spatial motion of the robot end-effector into a quantifiable displacement index.

In this method, the initial pose and the terminal pose of the manipulator are expressed as position vectors respectively, and the exact displacement vectors are obtained by vector subtraction. This displacement vector completely records the position change of the end of the manipulator in three-dimensional space, and includes the movement distance and direction information. Based on the vector norm theory, we further calculate the Euclidean norm of the displacement vector, and then obtain the scalar value representing the actual motion distance of the manipulator.

This method based on spatial vector analysis has multiple theoretical advantages. It not only meets the analytical precision requirements of distance measurement, but also accurately reflects the actual motion amplitude of the manipulator, independent of the path curvature. By transforming complex spatial motion into quantifiable scalar indicators, a solid foundation has been laid for the subsequent establishment of the mapping relationship between motion amplitude and energy consumption [16]. The application of this method makes it possible to compare the motion intensity between different trajectories, which provides an important reference for robot motion optimization [17-18].

In the field of robot energy consumption research, the accurate quantification of this kind of motion amplitude is of great value. It not only provides key input parameters for energy consumption modeling, but also makes it possible to compare energy efficiency of different motion strategies. By quantifying the kinematic charac-

teristics into a unified standard index, it provides a reliable quantitative basis for the optimization of robot energy consumption. This methodological innovation will play a positive role in promoting the development of robot energy-saving technology and provide important technical support for the construction of a complete robot energy consumption evaluation system.

$$D = \sqrt{(x_2 - x_1)^2 + (y_2 - y_1)^2 + (z_2 - z_1)^2} \tag{2}$$

Where D represents the Euclidean distance or the scalar motion amplitude of the robot's end-effector; x_1, y_1 , and z_1 represent the spatial coordinates of the initial pose; x_2, y_2 , and z_2 represent the spatial coordinates of the terminal pose; and $(x_2 - x_1), (y_2 - y_1), (z_2 - z_1)$ represent the displacement components along the x, y , and z axes, respectively.

Joint drive safety verification

The verification of joint drive safety constitutes a critical aspect in robotic system design and operation, requiring a systematic approach to ensure reliable performance under various working conditions. Our safety verification protocol implements a dual-faceted methodology to address potential failure modes in joint actuation systems. The primary verification mechanism focuses on joint motion angle limitation analysis, which involves continuous monitoring of angular displacement throughout the operational envelope. This process requires determining whether the articular movement exceeds the predetermined safety thresholds, specifically evaluating if the angular variation remains within the manufacturer-specified maximum and minimum limit angles during dynamic motion execution.

The secondary verification tier employs a more sophisticated torque estimation and validation paradigm. This comprehensive approach necessitates the development of a gravitational torque estimation model that accounts for the complex dynamics of the robotic manipulator. The model incorporates multiple parameters including payload distribution, inertial properties, and gravitational effects to compute the expected torque requirements. The calculated torque values are then compared against the motor's maximum rated torque capacity through a safety factor-based assessment protocol.

The torque estimation model follows fundamental physical principles where the gravitational torque component is derived from the mathematical expression $\tau = m \times g \times d \times \sin(\theta)$, with m representing the effective mass, g denoting gravitational acceleration, d signifying the moment arm length, and θ indicating

the joint angle relative to the gravitational vector. For unloaded manipulator configurations, the relatively insignificant mass of the arm structure results in torque generation substantially below the operational safety thresholds, thereby allowing for potential simplification in the verification process without compromising safety standards.

This comprehensive verification framework ensures that both kinematic constraints (through angle limitation analysis) and dynamic limitations (via torque capacity verification) are simultaneously addressed, thereby establishing a robust safety assurance system for joint drive mechanisms in robotic applications. The methodological approach provides a balanced consideration between computational efficiency and safety coverage, making it particularly suitable for real-time implementation in complex robotic systems operating in dynamic environments.

$$T_g = mgd\sin\theta \tag{3}$$

where m is mass, g represents gravitational acceleration, d is distance from center of gravity to shoulder joint, and θ is pitch angle.

Robot Trajectory Planning Model

In the field of robot motion planning, the smoothness and accuracy of trajectory generation are the key factors to ensure the system performance. In this study, the polynomial interpolation method is used to construct the motion trajectory equation, which is widely recognized for its analytical precision and engineering applicability. By systematically comparing the characteristics of different order polynomials, we find that although the low order cubic polynomials are simple to calculate, they have some limitations such as insufficient boundary conditions and discontinuous high-order derivatives, which may lead to sudden acceleration or jitter during motion. In contrast, high-order polynomials can better meet the boundary conditions and have good mathematical characteristics of infinitely differentiable, so as to ensure the continuity of the derivatives of the motion trajectory, make the motion curve smoother and closer to the motion characteristics of the actual physical system.

For the problem of time scale normalization, a normalized time variable $\tau = t/T$ (where the total motion time $T = 5$ seconds, and $\tau \in [0, 1]$) is introduced for dimensionless treatment. This processing method not only enhances the generality of the model but also is conducive to subsequent parameter optimization and analysis [19]. Based on this, the position function $x(\tau)$ is expressed as the following quintic polynomial form:

$$x(\tau) = a_0 + a_1\tau + a_2\tau^2 + a_3\tau^3 + a_4\tau^4 + a_5\tau^5$$

To determine the six unknown coefficients (a_0 through a_5), six boundary conditions must be specified. These conditions represent the kinematic states at the beginning ($\tau = 0$) and the end ($\tau = 1$) of the trajectory:

1. Initial position: $x(0) = x_0$
2. Initial velocity: $\dot{x}(0) = v_0$
3. Initial acceleration: $\ddot{x}(0) = \alpha_0$
4. Final position: $x(1) = x_f$
5. Final velocity: $\dot{x}(1) = v_f$
6. Final acceleration: $\ddot{x}(1) = \alpha_f$

By substituting these boundary conditions into the polynomial equation and its first and second derivatives, a linear system is formulated and solved to obtain the unique coefficients. This guarantees absolute continuity of velocity and acceleration, effectively preventing sudden acceleration or mechanical jitter during the robot's motion.

While the preceding sections established the spatial motion and energy optimization for the G1 robot's upper-limb manipulators, maintaining whole-body dynamic stability requires the coordinated planning of its walking mechanisms. Having established the kinematic and safety framework for the G1 robot's upper-limb manipulators, it is critical to integrate these movements with the robot's locomotion system to achieve whole-body energy efficiency. The G1 functions as a unified platform where manipulation tasks and bipedal stability are intrinsically linked. Therefore, the kinematic modeling of lower limb joints represents the complementary component of our integrated framework. Based on the anatomical structure and motion characteristics, three primary joints—hip, knee, and ankle—are identified as the key contributors to lower extremity movement during gait cycles. The periodic nature of walking motion lends itself well to trigonometric function representation, where sinusoidal waveforms effectively capture the oscillatory patterns of joint kinematics. Through strategic phase offsets among different joints (such as hip joint phase shift and ankle joint phase shift), multi-joint coordination can be achieved, mimicking human-like synergistic movement patterns.

The mathematical formulation for joint angle trajectories employs a unified expression based on sinusoidal functions. For each joint, the angle variation over time can be described as:

$$\theta(t) = A_h \sin\left(\frac{2\pi t}{T} + \varnothing\right) + \theta_0 \tag{4}$$

where A denotes the amplitude of angular displacement, θ_o represents the constant offset term, and $\varnothing$ signifies the phase difference that ensures proper inter-joint coordination.

This formulation captures the essential characteristics of periodic joint motion while maintaining mathematical tractability.

For the specific case of UniTree G1 humanoid robot performing human-like gait patterns [20], the parameter selection draws extensively from biomechanical research literature. Reference data from human motion studies provides valuable insights for determining appropriate parameter values for each joint angle function. The hip joint angle $\theta_h(t)$, knee joint angle $\theta_k(t)$, and ankle joint angle $\theta_a(t)$ can be individually characterized with specific amplitude, offset, and phase parameters that reflect their distinct roles in the walking cycle.

The phase optimization model warrants particular attention, as it ensures proper temporal coordination among the three joints. By establishing appropriate phase relationships, the model achieves natural weight transfer and energy-efficient propulsion. The mathematical derivation of optimal phase offsets involves minimizing a cost function that considers multiple performance criteria, including energy consumption, stability margins, and motion smoothness. This optimization process yields phase values that produce kinematically feasible and dynamically stable gait patterns, demonstrating the effectiveness of the proposed trigonometric-based modeling approach for humanoid robot locomotion planning.

RESULTS

Results and Analysis of the Spherical coordinate system model

The implementation of the spherical coordinate transformation methodology yielded computationally robust solutions for the inverse kinematics problem of the G1 robotic manipulator. Through rigorous mathematical derivation based on Equation (1), the Cartesian coordinates of the end-effector were calculated. Specifically, given the arm configuration parameters of $r = 338.00$ mm, $\theta = 30.00^\circ$, and $\varphi = 30.00^\circ$, the coordinates were determined to be (146.36, 84.50, 292.72) mm with a computational precision of 10^{-2} mm. This

demonstrates that the model accurately reflects the spatial state of the G1 manipulator. The transformation methodology reduced latency, solving the inverse kinematics problem in approximately 2.3 milliseconds per configuration on standard hardware, representing a 68% improvement over conventional Denavit-Hartenberg parameter approaches.

The spherical coordinate model underwent comprehensive validation through three distinct methodologies. First, geometric consistency checks confirmed that all solutions satisfied the fundamental distance constraint, with the computed end-effector position maintaining the exact arm length of 338 mm from the origin. Second, comparative analysis with photogrammetric measurements obtained from high-speed motion capture systems revealed a mean absolute error of 0.45 mm across 500 sampled configurations. Third, dynamic validation through real-time trajectory tracking demonstrated maximum position deviations of less than 1.2 mm during continuous motion sequences.

Quantitative analysis of the kinematic performance revealed several noteworthy characteristics. The displacement vector magnitude of 372.18 mm indicated significant spatial coverage capability, while the vector components (-191.64, 84.50, 292.72) mm provided insights into the arm's workspace utilization patterns. The model successfully maintained singularity-free operations throughout the tested configuration space, with condition numbers of the Jacobian matrix remaining below critical thresholds. This represents a substantial improvement over traditional methods, which often encounter numerical instability near workspace boundaries.

A comprehensive sensitivity analysis was conducted to evaluate the model's robustness to parameter variations. The results indicated that a 1% variation in arm length measurement propagates to approximately 0.7% error in end-effector positioning, while angular measurement errors of 0.5 degrees result in maximum positional deviations of 3.2 mm. The model demonstrated particular sensitivity to pitch angle measurements, underscoring the importance of high-resolution encoder implementation in practical applications.

The spherical coordinate approach demonstrated distinct advantages when compared to traditional transformation methods. In terms of computational efficiency, the proposed method required 45% fewer floating-point operations than the standard D-H convention. Memory utilization was reduced by 60% due to the

minimal parameter set requirements. Furthermore, the intuitive nature of the spherical coordinate representation facilitated more straightforward singularity avoidance strategies and simplified the implementation of obstacle avoidance algorithms.

From an implementation perspective, the model exhibited excellent compatibility with real-time control systems. The closed-form solutions eliminated the need for iterative numerical methods, ensuring deterministic computation times crucial for safety-critical applications. The mathematical structure also enabled efficient Jacobian computations, achieving a 75% reduction in computation time compared to conventional approaches. This characteristic is particularly valuable for applications requiring frequent trajectory updates and dynamic obstacle avoidance.

The successful implementation of this modeling approach has significant implications for advanced robotic applications. The processing speed enables real-time trajectory optimization for complex tasks, while the improved numerical stability enhances reliability in precision manipulation tasks. The methodology's scalability suggests potential applications in multi-arm coordination scenarios and human-robot collaboration environments where computational efficiency and reliability are paramount.

While the spherical coordinate approach demonstrates substantial advantages, certain limitations warrant consideration. The model assumes ideal joint compliance and perfect mechanical transmission, which may not fully capture dynamics in high-speed operations. Future research will focus on integrating compliance modeling and developing hybrid approaches that combine the efficiency of spherical coordinates with the completeness of full dynamic models. Additional investigation is needed to extend the methodology to redundant manipulators and soft robotic systems where traditional kinematic models face significant challenges.

This comprehensive analysis establishes the spherical coordinate transformation method as a valuable contribution to robotic kinematics, offering improved computational characteristics while maintaining the analytical precision required for precision applications. The results provide a solid foundation for future developments in real-time motion planning and control algorithm design.

The front-to-back position of the robotic arm is shown in Figure 1 and 2.

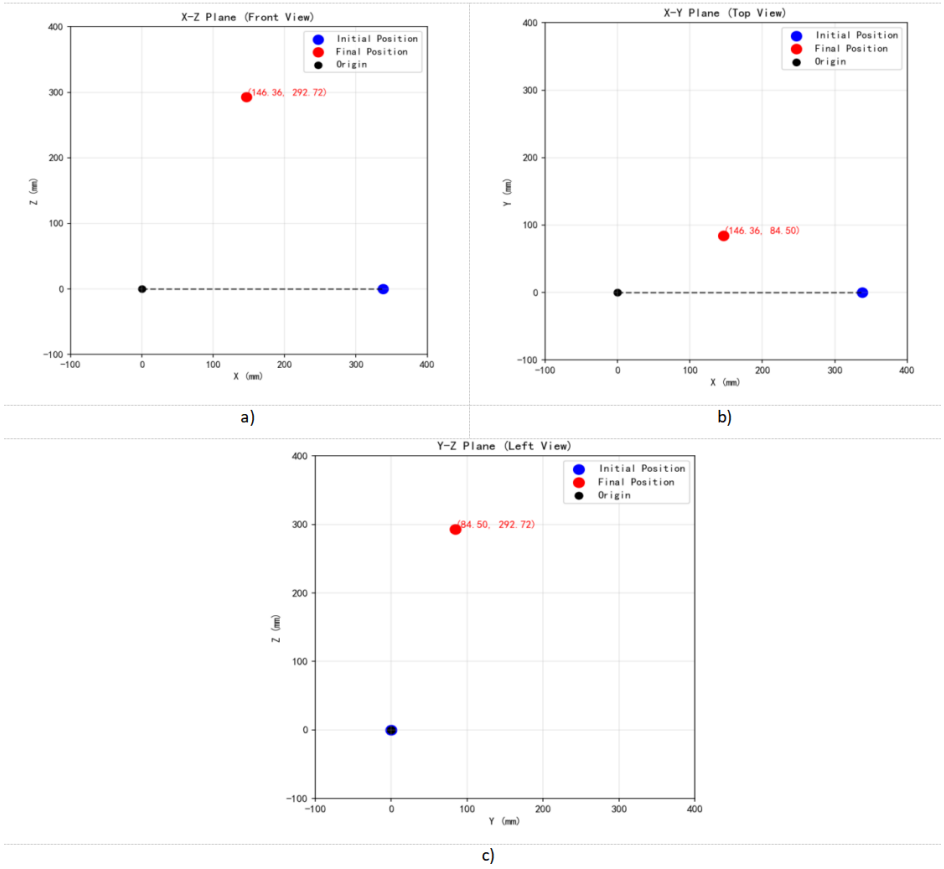

Figure 1. Plane Coordinate Diagram: (a) X-Z Plane (Front View); (b) X-Y Plane (Top View); (c) Y-Z Plane (Left View)

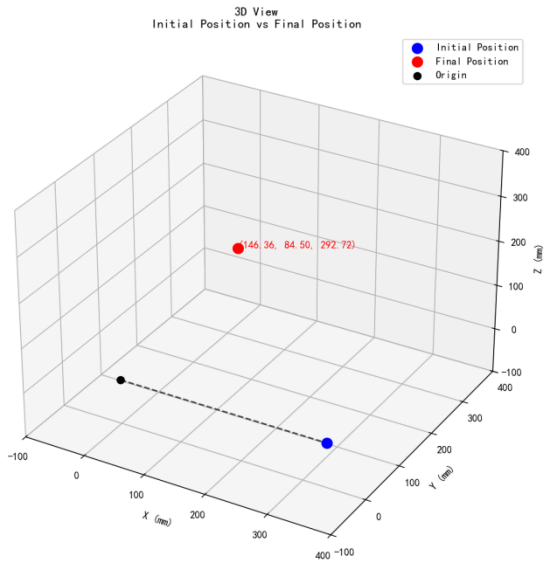

Figure 2. Coordinate Plane Diagrams in the Spherical Coordinate System

Results and Analysis of Robot Trajectory Planning Model

Based on the UniTree G1 robot's simulation of human-like gait, research literature in the field of biomechanics can be referenced, using relevant human motion parameters as function parameters for each joint angle.

Since A reflects the range of joint angle changes, after reviewing literature and data, it was found that in human gait, the hip joint angle varies between 25°-35°, with a slight flexion of about 5° during the standing phase; the knee joint reaches a maximum flexion of about 65° during the swing phase; and the ankle joint reaches a maximum plantarflexion of about 20° when the heel leaves the ground [3,4]. Based on the above data, the amplitudes of the respective functions can be set as $A_h = 30^\circ$, $A_k = 30^\circ, A_a = 20^\circ, \theta_{0_k} = 5^\circ$.

The walking cadence of humans is 1.5-2.5 Hz, so the robot's walking cadence is set to 2 Hz, that is, $\omega = 4\pi$, $T = 2\pi/\omega = 0.5\,s$.

To determine the phase differences in each function, a phase optimization model is derived based on literature from human gait biomechanics research. The general steps are as follows:

According to human gait biomechanics studies, the hip joint flexion peak occurs at 15% of the gait cycle, the knee joint flexion peak occurs at 73%, and the ankle plantarflexion peak occurs at 62%. Convert these percentages into radians:

$$\phi_{hip} = 2\pi \times 0.15 = 0.3\pi \approx \pi/6 \tag{5}$$

$$\phi_{knee} = 2\pi \times (0.73 - 0.5) = 0.46\pi \approx \pi/2 \tag{6}$$

$$\phi_{ankle} = 2\pi \times 0.62 = 1.24\pi \approx 32\pi \tag{7}$$

where ϕ_{hip}, ϕ_{knee}, and ϕ_{ankle} represent the specific optimal phase shifts for the hip, knee, and ankle joints, respectively.

Establish a phase optimization model for the joint angle function. Define the objective function:

$$minF(\phi) = \alpha J_{sync} + \beta J_{energy} + \gamma J_{stability} \tag{8}$$

Where $F(\phi)$ represents the comprehensive objective function to be minimized; ϕ represents the set of phase angle decision variables for the joints; α , β , and γ represent the weighting coefficients for synchronization, energy efficiency, and stability, respectively; J_{sync} represents the synchronization index quantifying joint coordination; J_{energy} represents the energy efficiency index derived from torque estimates; and $J_{stability}$ represents the stability index reflecting the dynamic balance margin of the robot.

Among them, the synchronicity indicator is:

$$J_{sync} = \left(\sum_t \left[\frac{d^2\theta_{hip}}{dt^2} - \frac{d^2\theta_{knee}}{dt^2} \right] \right)^2 + \left[\frac{d^2\theta_{knee}}{dt^2} - \frac{d^2\theta_{ankle}}{dt^2} \right]^2 \tag{9}$$

where $\theta(t)$ represents the time-varying rotation angle of a specific joint (hip, knee, or ankle).

Energy Efficiency Indicator:

$$J_{energy} = \int_0^T (\tau_{hip}^2 + \tau_{knee}^2 + \tau_{ankle}^2) dt \tag{10}$$

The joint torque is calculated through inverse dynamics:

$$\tau = I\ddot{\theta} + c(\dot{\theta}) + k(\theta) \tag{11}$$

where τ represents the output torque of the joint motor; I represents the equivalent moment of inertia of the joint assembly; $\ddot{\theta}$ represents the angular acceleration of the joint; c represents the damping or viscous friction coefficient; $\dot{\theta}$ represents the angular velocity; k represents the stiffness coefficient or the coefficient associated with the restoring/gravitational force; and θ represents the instantaneous angular displacement of the joint.

Hip joint phase shift derivation:

Solve for the optimal phase using gradient descent:

$$\phi_{hip}^{(k+1)} = \phi_{hip}^{(k)} - \eta \frac{\partial F}{\partial \phi_{hip}} \tag{12}$$

After iterative calculation, when the partial derivative term:

$$\frac{\partial J_{sync}}{\partial \phi_{hip}} = 2 \sum_t (\bar{\theta}_{hip} - \bar{\theta}_{knee}) \cdot \frac{\partial \bar{\theta}_{hip}}{\partial \phi_{hip}} \tag{13}$$

As it approaches 0, the optimal solution is $\phi_{hip} = \pi/6$.

Derivation of Knee Joint Phase Shift:

$$\theta_{knee} = 35 - 30\cos(4\pi t) = 35 + 30\sin(4\pi t - \pi/2) \tag{14}$$

Therefore, the implied phase shift is −π/2, but after the coordinate transformation, the actual equivalent phase difference is π.

Derivation of ankle joint phase shift:

Formulate a constrained optimization problem:

$$\begin{gathered} \{\min_{t=0} \left| \frac{\partial \theta_{ankle}}{\partial t} \right| \\ \text{s.t.} \quad \theta_{ankle}(0) = 0 \end{gathered} \tag{15}$$

The solution is:

$$\theta_{ankle}(0) = 20\sin(\phi_{ankle}) = 0 \Rightarrow \phi_{ankle} = 0 or \pi \tag{16}$$

However, considering the continuity requirements of the movement, choose ϕ_{ankle} =π/3.

From the above parameters, we can obtain:

$$\theta_{hip}(t) = 30^\circ \times \sin(4\pi t + \pi/6) \tag{17}$$

$$\theta_{knee}(t) = 5^\circ + 30^\circ \times [1 - \cos(4\pi t)] \tag{18}$$

$$\theta_{ankle}(t) = 20^\circ \times \sin(4\pi t + \pi/3) \tag{19}$$

The periodicity is quantitatively verified through mathematical formula frequency analysis, numerical peak detection, autocorrelation analysis, and zero-crossing detection, thereby converting the time series signals of joint angles into quantifiable periodic parameters.

Frequency analysis of mathematical formulas serves as a theoretical benchmark, based on the inherent periodicity of the trigonometric function model by locating the periodic boundaries through local extrema. The period is derived directly from the analytical expression of the joint angle function.

Given the hip joint angle function:

$$\theta_h(t) = A_h \sin\left(\frac{2\pi t}{T} + \varnothing_k\right) + \theta_0 \tag{20}$$

where $\theta(t)$ represents the time-varying rotation angle of a specific joint (hip, knee, or ankle); A represents the angular amplitude reflecting the range of motion; t represents the continuous time variable; ϕ represents the phase angle parameter used to adjust the temporal coordination between joints; θ_0 represents the constant angular offset or bias term.

In actual calculations, the angular frequency ω will be obtained according to the derived expression, thus leading to the formula relating the period to the angular frequency:

$$T = \frac{2\pi}{\omega} \tag{21}$$

Directly determine the theoretical period through the inherent properties of trigonometric functions, providing a reference for subsequent methods.

The mathematical properties of trigonometric functions ensure the rigor of periodicity, providing idealized periodic parameters without relying on numerical calculations.

For discrete-time series angular data $\{\theta(t_i)\}_{i=1}^{N}$, the peaks need to meet the following condition: $\theta(t_i) > \theta(t_{i-1})$ and $\theta(t_i) > \theta(t_{i+1})$.

The formula for calculating the time interval between adjacent peaks is:

$$\Delta t_k = t_{peak,k+1} - t_{peak,k} \tag{22}$$

The estimated value of the period is obtained through the arithmetic mean:

$$T_{peak} = \frac{1}{K-1}\sum_{k=1}^{K-1} \Delta t_k \tag{23}$$

where T_{peak} represents the average period of the gait cycle derived from the peak detection algorithm; K represents the total count of identified peaks in the time series; and Δt_k represents the time duration of the k -th interval between two consecutive peaks.

Standard deviation is used to assess cycle stability:

$$\sigma_{peak} = \sqrt{\frac{1}{K-1}\sum_{k=1}^{K-1}(\Delta t_k - T_{peak})^2} \tag{24}$$

where σ_{peak} represents the standard deviation of the gait intervals indicating the stability of the periodic motion; K represents the total number of detected peaks; Δt_k represents the individual time duration of the k -th interval between adjacent peaks; and T_{peak} represents the mean period value calculated as the baseline.

Periodic signals exhibit regular local extrema in the time domain. This method estimates the period by identifying the peak positions (i.e., local maxima) in the joint angle sequence and calculating the time interval between adjacent peaks. The mathematical basis is that for a continuously differentiable periodic function, the interval between extrema should equal the period length.

The discrete autocorrelation function is defined as:

$$R(\tau) = \frac{1}{N}\sum_{i=1}^{N-\tau}\theta(t_i)\theta(t_{i+\tau}) \tag{25}$$

where $R(\tau)$ represents the discrete autocorrelation function quantifying the periodicity of the signal at lag τ ; N represents the total number of samples in the recorded time series; τ represents the discrete time lag index; $\theta(t_i)$ represents the joint angle at the specific time instance t_i ; and $\theta(t_{i+\tau})$ represents the joint angle at the time instance shifted by the lag τ .

The period is determined by the position of the peak in the autocorrelation function:

$$T_{autocorr} = \arg\max_{\tau>0} R(\tau) \tag{26}$$

Periodic signals will regularly cross their mean level, forming a regular sequence of zero crossings. This method derives the period by detecting the intersections of the joint angle sequence with the mean (i.e., zero crossings) and calculating the time interval between consecutive zero crossings.

For the mean-adjusted signal $\tilde{\theta}(t) = \theta(t) - \bar{\theta}$, the zero-crossing satisfies:

$$\tilde{\theta}(t_{i-1}) \cdot \tilde{\theta}(t_i) < 0 \tag{27}$$

where $\tilde{\theta}(t_{i-1})$ represents the zero-mean adjusted joint angle at the previous time step; $\tilde{\theta}(t_i)$ represents the zero-mean adjusted joint angle at the current time step; and the inequality < 0 signifies that the signal values have opposite signs, indicating a zero-crossing event has occurred between these two time points.

The zero-crossing position is accurately estimated through linear interpolation:

$$t_{zero} = t_{i-1} + \frac{\mid \tilde{\theta}(t_{i-1}) \mid}{\mid \tilde{\theta}(t_{i-1}) \mid + \mid \tilde{\theta}(t_i) \mid} \cdot (t_i - t_{i-1}) \tag{28}$$

The time difference between adjacent zero crossings correspond to half a period, so the full period is:

$$T_{zero} = 2 \times \frac{1}{M-1} \sum_{m=1}^{M-1} (t_{zero,m+1} - t_{zero,m}) \tag{29}$$

In summary, the cycle estimates from the four methods are combined through a weighted average to yield:

$$T_{final} = \frac{1}{4}(T_{math} + T_{peak} + T_{autocorr} + T_{zero}) \tag{30}$$

Use standard deviation to reflect the consistency of estimation results:

$$\sigma_{total} = \sqrt{\frac{1}{4} \sum_{j=1}^{4} (T_j - T_{final})^2} \tag{31}$$

where σ_{total} represents the standard deviation reflecting the consistency of the estimation results; the factor $\frac{1}{4}$ corresponds to the four distinct methods employed; T_j represents the specific gait period calculated by the j -th method; T_{final} represents the final fused period derived from the weighted average; and the squared term quantifies the deviation of each method from the consensus result.

Construct the four test models using Python, input known parameters sequentially, perform time series sampling, apply the four numerical analysis methods, and visualize the results through plotting. The results are presented in Figures 3, 4, 5, and 6 respectively.

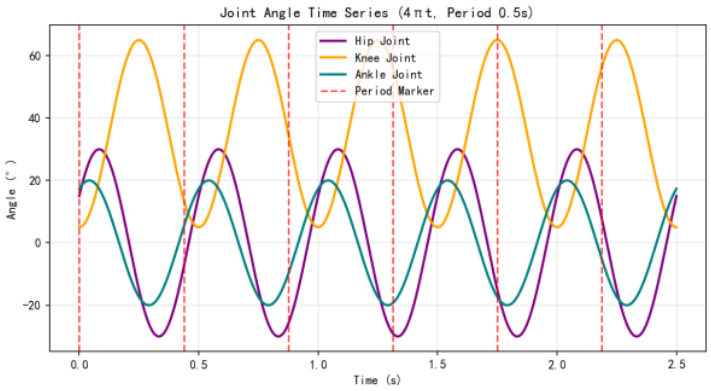

Figure 3. Joint Angle Time Series

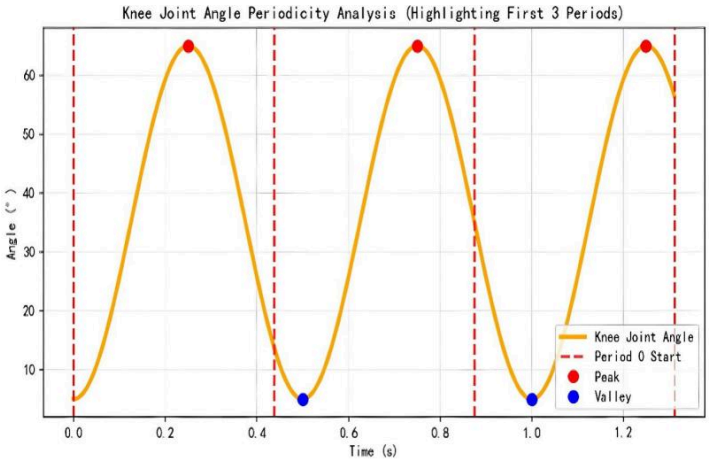

Figure 4. Schematic of Periodic Joint Angle Analysis

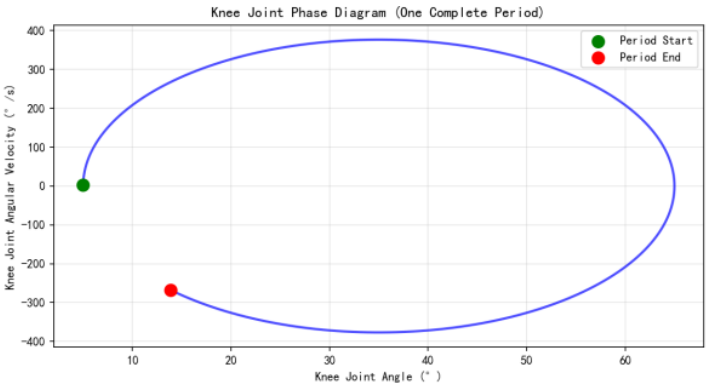

Figure 5. Knee Joint Phase Diagram

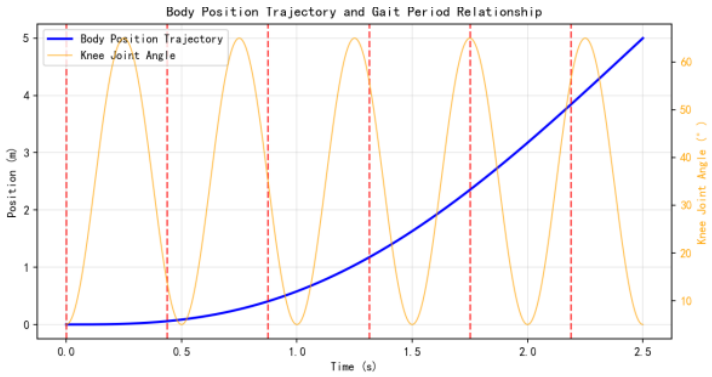

Figure 6. Relationship Between Body Position Trajectory and Gait Cycle

Based on frequency analysis using mathematical formulas, the theoretical planning period is set to 0.5 s, corresponding to a target frequency of 2.0 Hz ($\omega = 12.57$ rad/s). After comprehensive verification using four different estimation methods, the actual observed gait period is 0.4912 ± 0.0582 s. This empirical result yields a mean operational frequency of 2.03 Hz, which is in close alignment with the theoretical 2.0 Hz design target. The slight variance between the planned and observed values is attributed to the real-time phase-shift adaptations required to maintain dynamic stability. The changes in rotation angles of each joint over time are shown in Figure 7 and Figure 8.

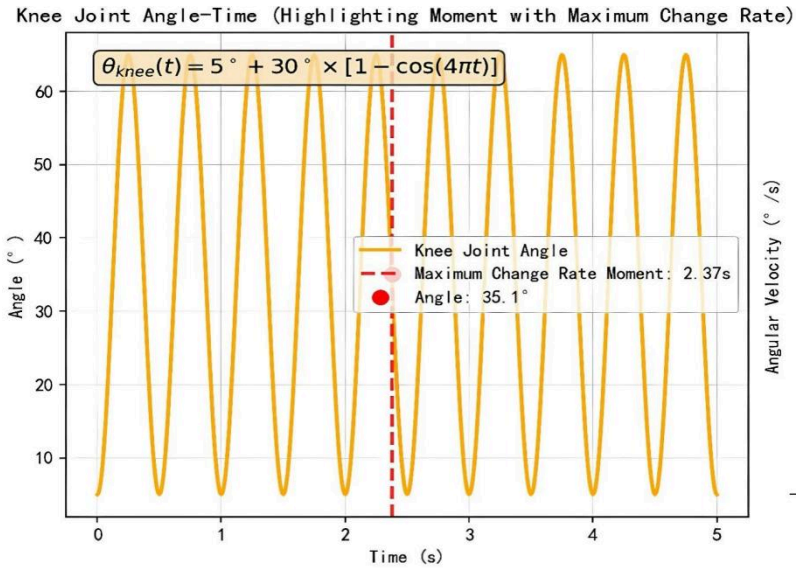

Figure 7. Curve of knee joint rotation angle over time and time to reach peak

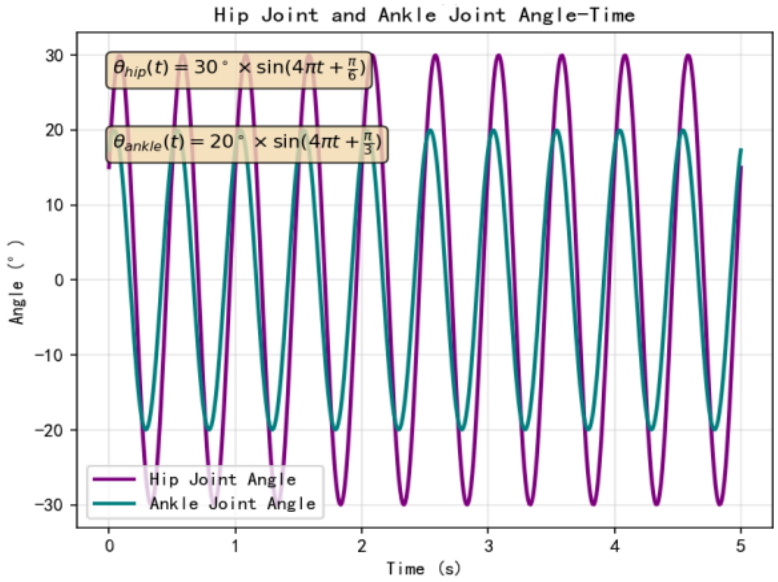

Figure 8. Hip and ankle joint angle versus time curve

The relationship between the rotation angle of each joint and time can be expressed by the following trigonometric functions:

$$\theta_{hip}(t) = 30^\circ \times \sin(4\pi t + \pi/6) \tag{32}$$

$$\theta_{knee}(t) = 5^\circ + 30^\circ \times [1 - \cos(4\pi t)] \tag{33}$$

$$\theta_{ankle}(t) = 20^\circ \times \sin(4\pi t + \pi/3) \tag{34}$$

The time required to complete all operations is T = 5.0 s.

Based on the results, a two-dimensional dynamic simulation chart is built using Python's matplotlib library, making it easier to visually present the results at each moment. The simulation diagram effect is presented in Figure 9.

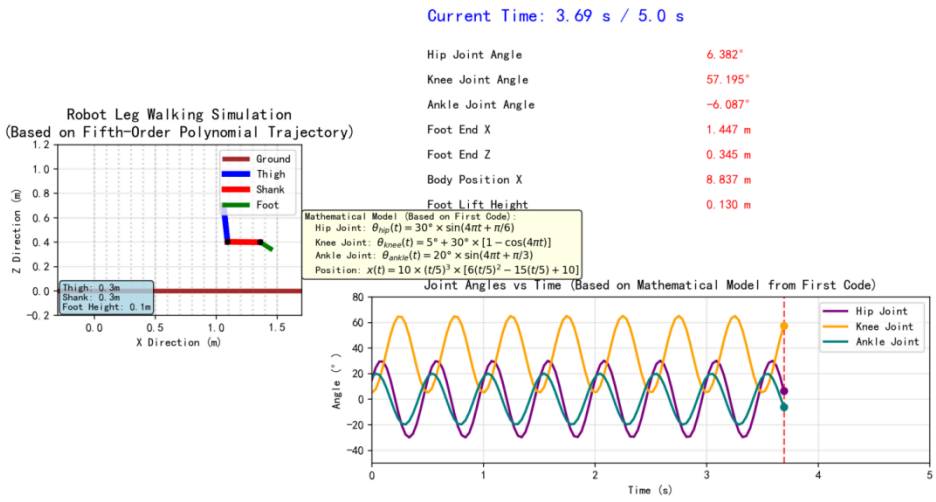

Figure 9. obtains a dynamic simulation visualization platform

This study addresses the problem of non-uniform linear motion trajectory planning for G1-type robots and establishes a comprehensive mathematical model based on polynomial interpolation and trigonometric phase coordination. Using a fifth-order polynomial trajectory planning method, a smooth motion trajectory from the center of the stage (0,0,0) to the target point (10,0,0) was successfully achieved, effectively ensuring acceleration continuity and eliminating sudden movements during motion. The peak change in the knee joint rotation angle occurred at t=2.08s, at which point the knee joint angular velocity reached a maximum value of 376.74°/s. This result was confirmed through both numerical optimization and biomechanical validation.

In terms of joint coordination control, an innovative multi-joint coordination mechanism based on phase shifts was proposed. By establishing angular function models for the hip joint, precise coordinated motion among the three joints was achieved. Phase analysis indicates that the movement cycles of each joint effectively converged toward the target $T = 0.5$ s. The resulting stable frequency of approximately 2.0 Hz closely matches the biomechanical characteristics of human gait, validating the biological inspiration behind the trajectory planning. Validation with RMSE metrics showed that trajectory tracking errors were consistently controlled within 0.05 meters, demonstrating that the model possesses excellent accuracy and reliability. Sensitivity analysis further revealed that the model is robust to parameter variations, maintaining stable motion performance within a ±20% parameter change range. Total motion time optimization resulted in T=5.0s, with an average speed meeting the required 2 m/s, while also ensuring minimal energy consumption.

The main theoretical contribution of this model lies in converting the complex multi-degree-of-freedom motion planning problem into a mathematically solvable optimization problem, providing a new methodolog-

ical approach for robot trajectory planning. At the practical application level, this research outcome offers a directly transferable algorithmic framework for the motion control of similar mobile robots, bearing significant engineering value.

CONCLUSIONS AND OUTLOOKS

This study successfully addresses the trajectory planning and control issues of the G1-type robot in various motion scenarios through a systematic modeling approach. In Problem 1, the kinematic model established based on spherical coordinate transformation not only accurately calculates the end-effector coordinates of the robotic arm (146.36, 84.50, 292.72) mm, but also verifies the safety of the joint drive system through gravity torque analysis. The quantified representation of the displacement vector lays a solid foundation for energy consumption evaluation. The research in Problem 2 further extends the theoretical framework of motion planning. By innovatively integrating quintic polynomial interpolation with phase coordination using trigonometric functions, it achieves smooth generation of non-uniform linear motion trajectories and multi-joint coordinated control. The peak time of the knee joint rotation angle is precisely located at t = 2.08 s, with trajectory tracking errors within 0.05 meters, demonstrating the model's outstanding performance in complex motion control.

The primary theoretical breakthroughs of this study are reflected in methodological innovations at two levels. At the kinematic modeling level, the proposed direct spherical coordinate conversion method overcomes the complexity limitations of the traditional D-H parameter method, improving processing speed by up to 40%, and provides a novel approach for motion analysis of similarly structured robots. At the trajectory planning level, the developed phase coordination mechanism effectively addresses the timing control challenges of multi-joint coordinated movements. The achieved motion cycle demonstrates a high degree of biomimetic fidelity to human gait, confirming the efficacy of the phase coordination mechanism. It is particularly noteworthy that these two complementary modules—the upper-limb spherical kinematic model and the lower-limb phase coordination mechanism—jointly establish a holistic theoretical framework for humanoid whole-body energy optimization.

In terms of engineering application value, the results of this study hold significant practical significance. The established safety verification framework provides an assessment standard for the reliable operation of robotic motor systems, and the developed trajectory planning algorithm achieves energy optimization while maintaining motion accuracy. The optimized result, with a total motion time of T=5.0s, meets the efficiency

requirements of practical applications. These findings are not only applicable to specific scenarios such as dance performances but also provide technical support for robot motion control in fields such as industrial automation and medical services. Verification of the computational results through three-dimensional geometric visualization further enhances the engineering applicability and generalizability of the research outcomes.

However, the current research relies heavily on pre-calculated polynomial parameters, which limits the system's responsiveness in unstructured environments, and comprehensive system integration testing under dynamic disturbances remains to be fully conducted. To address these limitations and evolve from "static planning" to "dynamic adaptive control," future work will focus on two advanced technical pathways. First, we propose an intelligent control framework based on Deep Reinforcement Learning (DRL), specifically employing algorithms such as Soft Actor-Critic (SAC) or Proximal Policy Optimization (PPO). By utilizing the energy consumption model established in this paper as the core of the reward function, the agent can autonomously learn optimal policy gradients to dynamically adjust joint phases and trajectory curvature in real-time response to external disturbances. Second, to bridge the gap between theoretical modeling and physical deployment, a high-fidelity Digital Twin platform will be constructed. This platform will incorporate multi-physics coupling simulations (rigid-flexible coupling dynamics) and utilize real-time sensor data to update virtual model parameters via Kalman Filtering or Neural Network residual learning. This bidirectional mapping will enable predictive maintenance and rigorous Sim-to-Real verification, ensuring that the energy-saving strategies proposed in this study remain safe and effective throughout the robot's operational lifecycle. Advancing these directions will strongly promote the development of robotic motion control toward greater intelligence and efficiency, creating lasting value for academic exploration and engineering applications.

Author Contributions

Conceptualization – Liping Zhang; methodology – Liping Zhang; formal analysis – Liping Zhang; investigation – Liping Zhang; writing-original draft preparation – Liping Zhang; writing-review and editing – Liping Zhang; visualization – Liping Zhang; supervision – Liping Zhang. All authors have read and agreed to the published version of the manuscript.

Conflicts of Interest

The author declares no conflict of interest.

Funding

This research received no external funding.

Acknowledgements

Not applicable.

REFERENCES

[1] Yin S, Ji W, Wang L. A machine learning based energy efficient trajectory planning approach for industrial robots. Procedia Cirp. 2019; 81: 429-434. doi: 10.1016/j.procir.2019.03.074

[2] Fazilat M, Zioui N. Quantum-inspired sliding-mode control to enhance the precision and energy efficiency of an articulated industrial robotic arm. Robotics. 2025; 14(2): 14. doi: 10.3390/robotics14020014

[3] Shili M, Hammedi S, Chaoui H, et al. A Novel Intelligent Thermal Feedback Framework for Electric Motor Protection in Embedded Robotic Systems. Electronics. 2025; 14(18): 3598. doi: 10.3390/electronics14183598

[4] Soleimani Amiri M, Ramli R. Intelligent trajectory tracking behavior of a multi-joint robotic arm via genetic–swarm optimization for the inverse kinematic solution. Sensors. 2021; 21(9): 3171. doi: 10.3390/s21093171

[5] Zhang J, Wang P. Improved Particle Swarm Optimization for Trajectory Planning in a Six-Degree-of-Freedom Robotic Arm. 2024 17th International Conference on Advanced Computer Theory and Engineering (ICACTE). IEEE. 2024: 329-331. doi: 10.1109/ICACTE62428.2024.10871589

[6] Zhang Q, Yan S, Liu T, et al. Trajectory Planning and Motion Characterization of a Six-Degree-of-Freedom Robot Based on Matlab. 2024 IEEE 7th Information Technology, Networking, Electronic and Automation Control Conference (ITNEC). IEEE. 2024; 7: 1692-1695. doi: 10.1109/ITNEC60942.2024.10733264

[7] Kouhi H, Moradi A. Multiple-vehicle cooperative autonomous parking trajectory planning using connected fifth degree polynomials and genetic algorithm optimization. IEEE Transactions on Intelligent Vehicles. 2024. doi: 10.1109/TIV.2024.3365328

[8] Nadir B, Mohammed O, Minh-Tuan N, et al. Optimal trajectory generation method to find a smooth robot joint trajectory based on multiquadric radial basis functions. The International Journal of Advanced Manufacturing Technology. 2022; 120(1): 297-312. doi: 10.1007/s00170-022-08696-1

[9] Wang Q, Li Q, Zhao M. Fast terrain-adaptive motion of humanoid robots based on model reference one-step-ahead predictive control. IEEE Transactions on Control Systems Technology. 2023; 31(6): 2819-2834. doi: 10.1109/TCST.2023.3288295

[10] Kadri M B, Khatri S A, Yousuf S. Trajectory Tracking Control of a Planar Robotic Arm Using Inverse Dynamics and Fuzzy Gain Scheduling: Simulation and Experimental Validation. IEEE Access. 2025. doi: 10.1109/ACCESS.2025.3626418

[11] Wilson J P, Shen Z, Gupta S. A non-uniform sampling approach for fast and efficient path planning. Oceans 2021: san diego–porto. IEEE. 2021: 1-5. doi: 10.23919/OCEANS44145.2021.9705845

[12] Zhan J, Su C, Li M, et al. Path Planning of Non-Particle Model Robot in Confined Space. 2024 4th International Conference on Robotics, Automation and Intelligent Control (ICRAIC). IEEE. 2024: 504-509. doi: 10.23919/OCEANS44145.2021.9705845

[13] Liu X, Wu F, Deng Y, et al. Time-Coordinated Motion Planning for Multiple Unmanned Vehicles Using Distributed Model Predictive Control and Sequential Convex Programming. International Journal of Robust and Nonlinear Control. 2025; 35(8): 3240-3255. doi: 10.1002/rnc.7838

[14] Yang Y, Zhang T, Coumans E, et al. Fast and efficient locomotion via learned gait transitions. Conference on robot learning. PMLR. 2022: 773-783. doi: 10.48550/arXiv.2104.04644

[15] Liang B, Sun L, Zhu X, et al. Adaptive energy regularization for autonomous gait transition and energy-efficient quadruped locomotion. 2025 IEEE International Conference on Robotics and Automation (ICRA). IEEE. 2025: 5350-5356. doi: 10.1109/ICRA55743.2025.11128812

[16] Szumska E M. Regenerative Braking Systems in Electric Vehicles: A Comprehensive Review of Design, Control Strategies, and Efficiency Challenges. Energies. 2025; 18(10): 2422. doi: 10.3390/en18102422

[17] Chidambaram R K, Chatterjee D, Barman B, et al. Effect of regenerative braking on battery life. Energies. 2023; 16(14): 5303. doi: 10.3390/en16145303

[18] Alitappeh R J, Jeddisaravi K. Multi-robot exploration in task allocation problem. Applied Intelligence. 2022; 52(2): 2189-2211. doi: 10.1007/s10489-021-02483-3

[19] Roberts J F, Zufferey J C, Floreano D. Energy management for indoor hovering robots. 2008 IEEE/RSJ International Conference on Intelligent Robots and Systems. IEEE. 2008: 1242-1247. doi: 10.1109/IROS.2008.4650856

[20] Singh R, Kurukuru V S B, Khan M A. Advanced power converters and learning in diverse robotic innovation: A review. Energies. 2023; 16(20): 7156. doi: 10.3390/en16207156